JOURNAL OF GEOPHYSICAL RESEARCH, VOL. 113, A12305, doi:10.1029/2008JA013308, 2008

Behavior of the F_2 peak ionosphere over the South Pacific at dusk during quiet summer conditions from COSMIC data

A. G. Burns,[1] Z. Zeng,[1,2] W. Wang,[1] J. Lei,[1,3] S. C. Solomon,[1] A. D. Richmond,[1] T. L. Killeen,[1] and Y.-H. Kuo[4]

Received 10 April 2008; revised 11 July 2008; accepted 3 September 2008; published 11 December 2008.

[1] The six-satellite Constellation Observing System for Meteorology, Ionosphere and Climate (COSMIC) mission makes routine ionospheric measurements over the entire globe using occultation techniques. These observations have been used in this study to develop global-scale climate maps of N_mF_2 and h_mf_2 during the southern (northern) summer (winter). Enhanced electron densities that appear to be associated with the southern, equatorial (Appleton) anomaly are displaced far southward at dusk and, within about an hour, form the Weddell Sea anomaly. Coincidentally, the height of the F_2 peak increases on the northern boundary of this anomaly. This height increase is also displaced southward as the enhanced electron densities are displaced southward, suggesting that the electron density increases are associated with the F_2 peak rising. As well as being an interesting phenomenon in its own right, this behavior may shed new light on the formation of the Weddell Sea anomaly. No unambiguous explanation for this behavior can be determined from the data presently available, but an examination of some possibilities suggests that an evening downward flux of plasma from the plasmasphere may be at least partly responsible for the phenomenon.

Citation: Burns, A. G., Z. Zeng, W. Wang, J. Lei, S. C. Solomon, A. D. Richmond, T. L. Killeen, and Y.-H. Kuo (2008), Behavior of the F_2 peak ionosphere over the South Pacific at dusk during quiet summer conditions from COSMIC data, *J. Geophys. Res.*, *113*, A12305, doi:10.1029/2008JA013308.

1. Introduction

[2] The Constellation Observing System for Meteorology, Ionosphere, and Climate (COSMIC) mission consists of six satellites that measure, among other things, code delays and phase advances associated with GPS occultations. This measurement involves calculating the along-track differential phase delay from a signal sent by the GPS satellites [*Rocken et al.*, 2000; *Lei et al.*, 2007] as it travels through the Earth's ionosphere and atmosphere near the horizon. The electron density at the tangent point can be calculated from this phase delay. Maps of variations in electron density have been built up for this paper using these data.

[3] Some earlier published studies showed that the climatology obtained from COSMIC ionospheric data [*Lei et al.*, 2007] behaved in a way that was similar to both ionosonde data and the IRI model [e.g., *Bilitza*, 2007] in magnitude and morphology. Other features that were also seen by *Lei et al.* [2007] included well-known ionospheric phenomena. For example, they saw the north-south asymmetry of the equatorial anomalies and variations in their longitudinal structure.

[4] A recent example of the behavior that can be deduced from these observations was given in a paper by *Zeng et al.* [2008]. They used the COSMIC data to study the nature and causes of the annual anomaly in F_2 peak electron densities and found that the National Center for Atmospheric Research–thermosphere-ionosphere-electrodynamics general circulation model (NCAR-TIEGCM) reproduced the COSMIC observations very well. They also found that the annual anomaly in electron density was primarily driven by the geometry of the Earth's magnetic field, but that the changing Sun-Earth distance did play a role as well. These studies and others show that COSMIC data is a valuable tool for climatological studies of the ionosphere during quiet conditions.

[5] Before describing the feature that is the center point of this paper it is worth describing the main features of the F_2 peak climatology [e.g., see *Rishbeth and Garriott*, 1969]. The dominant F_2 peak ion is O^+. This ion is primarily produced by the photoionization of O and it is lost through recombination with the neutral gases O_2 and N_2. As these gases are heavy, their densities decrease rapidly with height so the topside ionosphere reaches a quasi-equilibrium state as a result of ambipolar diffusion [e.g., *Jee et al.*, 2007]. Other transport processes are also important, including the ion drifts that are driven by ExB forcing near the magnetic equator and neutral winds pushing ions up field lines into

[1]High Altitude Observatory, National Center for Atmospheric Research, Boulder, Colorado, USA.
[2]Now at Department of Earth and Ocean Sciences, University of British Columbia, Vancouver, British Columbia, Canada.
[3]Now at Aerospace Engineering Sciences Department, University of Colorado, Boulder, Colorado, USA.
[4]Mesoscale and Microscale Meteorology Division, National Center for Atmospheric Research, Boulder, Colorado, USA.

0148-0227/08/2008JA013308$09.00

regions of less recombination or down field lines into regions of more recombination.

[6] A simple ionospheric pattern would occur if the horizontal structure of the neutral gases was uniform and the transport processes were not important: the F_2 peak ionosphere would have a circular pattern in which the electron densities decreased horizontally away from the subsolar point. This pattern is very similar to the pattern of electron densities that does exist in the F_1 region.

[7] In the actual ionosphere, transport processes, and variations in neutral composition and temperature, cause anomalies. The most famous of these anomalies are the equatorial or Appleton anomalies [e.g., *Rishbeth and Garriott*, 1969], which are two bands of enhanced electron densities that lie parallel to the magnetic equator and are centered at a geomagnetic latitude of about 20 degrees. They are prominent in the daytime and extend for a long time into the night. They are driven by the electric field at the magnetic equator and the subsequent redistribution of electron density.

[8] Another well-known feature of the ionosphere is the winter anomaly [e.g., *Rishbeth and Garriott*, 1969]. In this anomaly the daytime electron densities are greater in winter at middle latitudes than they are in summer. This anomaly is caused by the distribution of neutral composition. O densities are large in winter and relatively small in summer, whereas the molecular species have the opposite morphology. The balance between production and loss then causes the higher electron densities in winter.

[9] There is another anomaly in the climatological behavior of F_2 electron density which has been far less studied, but which was also been known for 50 years. This is the Weddell Sea anomaly [e.g., *Bellchambers and Piggott*, 1958; *Horvath*, 2006].

[10] The Weddell Sea anomaly was discovered as a result of a large number of ionospheric observatories being placed in Antarctica during the International Geophysical year in 1957. These data were analyzed by a number of researchers [e.g., *Bellchambers and Piggott*, 1958; *Penndorf*, 1965; *Dudeney and Piggott*, 1978], who noticed that a peculiar phenomenon occurred in the electron densities at the F_2 peak over the Weddell Sea region of Antarctica. They found that, in summer, electron densities were larger at night than during the daytime. No such anomaly occurred in this region in winter. A number of papers were written describing and attempting to explain this phenomenon. Explanations include transportation from the dayside by the ion convection pattern [*Penndorf*, 1965] and by neutral winds [*Dudeney and Piggott*, 1978]. Both mechanisms have issues. The former is problematic because, although the Weddell Sea is at high geographic latitudes, it is in the middle latitudes geomagnetically. Ion drifts are constrained by magnetic field lines and cannot readily transport plasma into the geomagnetic middle latitudes. The latter also has problems as the nighttime enhancement in the Weddell Sea anomaly always begins at dusk. The neutral winds that blow across the magnetic polar cap in an antisunward direction have a jet near midnight. They flow toward the Sun in the dusk region [e.g., see *Killeen and Roble*, 1988] and so this jet cannot produce the Weddell Sea anomaly. An alternative forcing mechanism may involve the day-to-night, solar EUV driven winds. This forcing mechanism could come into effect because the Weddell Sea region is normally separated from the high-latitude convection pattern. For this mechanism to work, equatorward winds have to blow ions up field lines into regions of less recombination. However, winds are mainly zonal at dusk in quiet geomagnetic times [e.g., *Dickinson et al.*, 1981; *Burns et al.*, 1995] and so this mechanism should also not contribute to increasing electron densities. It should be pointed out, though, that these results were ones that applied to the atmosphere in general and not specifically to the Weddell Sea region.

[11] Possible explanations involving neutral composition were dismissed by *Bellchambers and Piggott* [1958]. We also do not see any reason why there might be large neutral compositional variations in this region. Later we discuss why the current data from COSMIC is not compatible with an explanation involving neutral composition.

[12] In general, there seems to be no explanation at present for this anomaly. We will show later that this behavior is even more unusual than expected.

[13] Recent work by *Horvath* [2006] has described the morphology of the Weddell Sea anomaly using satellite data. Horvath used TOPEX/Poseidon data and gave a more complete morphology of the Weddell Sea anomaly than has hitherto been available, as much of the disturbance occurs over oceans from which ground-based observations are not available. This work showed that the anomaly is a large ($\sim$22 million square kilometers) feature that extends between 60 and 160°W longitude and peaks between 50 and 60°S latitude.

[14] The purpose of this paper is to present evidence for anomalous behavior of the F_2 electron densities in the low and middle latitudes of the South Pacific Ocean just after dark that leads to the formation of both the Weddell Sea anomaly and its extension across the aforementioned Ocean. Although we attempt to narrow down the possible causes of this behavior, there is insufficient evidence to provide a mechanism for its formation. The paper is organized in the following way. Section 2 briefly describes the COSMIC data and the analysis of this data needed to obtain the seasonal climatology. Section 3 describes the observations, section 4 discusses these results and section 5 is a conclusion section.

2. Data

[15] Six satellites, which are together called COSMIC, were launched on 15 April 2006 [*Kumar*, 2006]. Three different instruments make up their science payload. The instrument that interests us here is the advanced GPS receiver. It is used to make the atmosphere and ionosphere measurements through phase and Doppler shifts of radio signals. The phase advance is used to compute the amount of signal bending that occurs as the impact parameter varies [*Rocken et al.*, 2000]. This bending is then used to compute vertical profiles of refractivity. The refractivity is directly proportional to ionospheric electron densities when impact parameters are above 80 km [*Lei et al.*, 2007]. The Abel inversion technique is then applied to retrieve electron density profiles from the total electron content along these raypaths [*Hajj and Romans*, 1998; *Schreiner et al.*, 1999].

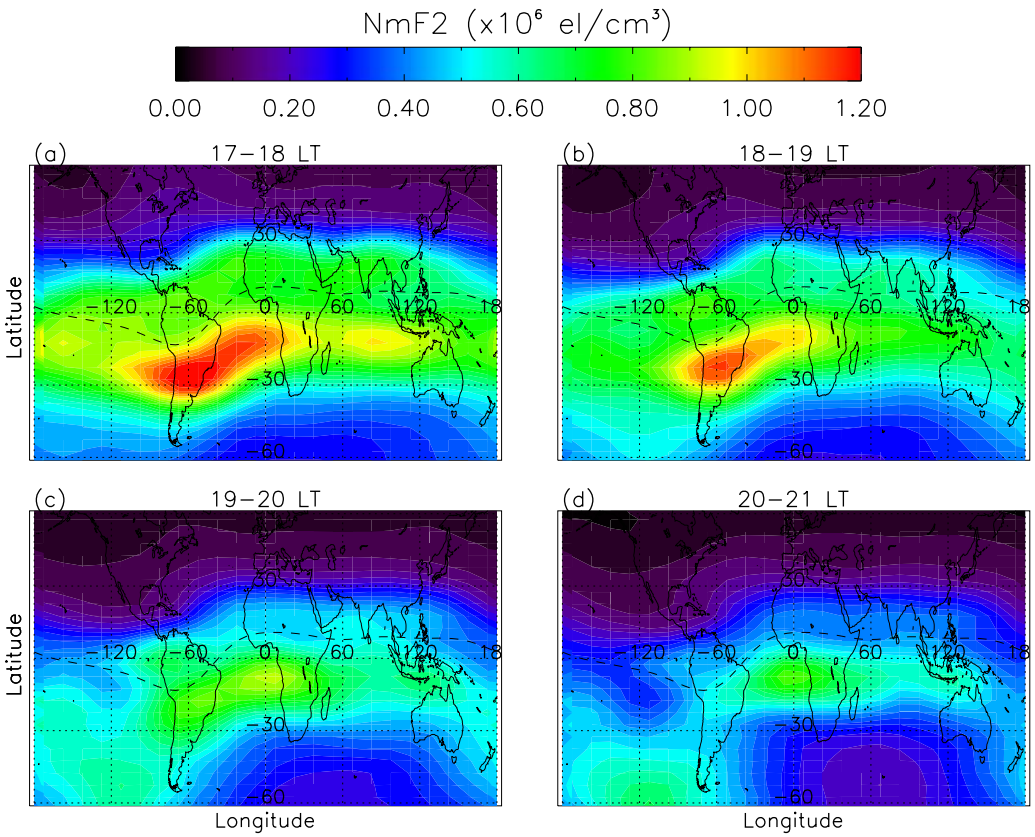

Figure 1. Global maps of N_mF_2 calculated from COSMIC data for four local time bands: (a) 1700–1800 local time, (b) 1800–1900 local time, (c) 1900–2000 local time, and (d) 2000–2100 local time.

[16] The satellites were launched from the same rocket and initially followed the same orbit track at 512 km. The satellites were then sequentially raised to orbits at 800 km. The time delay for this increase in elevation has been designed to spread the orbital planes, so the individual satellites are now 30 degrees apart. The COSMIC satellites now provide approximately 24 h of local time coverage globally and provide about 2500 vertical electron density profiles per day. The data used here come primarily from the period when the satellites were being maneuvered into this orbital configuration. Despite some lack of coverage from this intermediate configuration, local time, universal time, longitude and latitude coverage is mostly complete (see Figure 3). In the occasional case where it is not, the data are interpolated using the methodology described in the subsequent paragraph.

[17] The data used in this study were retrieved from the COSMIC (http://www.cosmic.ucar.edu) observations from launch until the August 2007. Disturbed conditions with a k_p index larger than 3 were removed during this solar minimum period. Abel inverted data [*Lei et al.*, 2007] were used in this study to obtain values for N_mF_2 and h_mf_2. The data were binned in a uniform horizontal grid with a resolution of 10° in geographic longitude and 5° in geomagnetic latitude. For each subset, the data are sorted in local time (LT) and a weighted average was applied [*Beers et al.*, 1990] with a 2 h sliding window and a 1 h moving step. The data were then separated into 91 day seasons centered on the solstices and the equinoxes. So the data used in this study were measured between 6 November 2006 and 7 February 2007. Finally, a seventh-order polynomial fitting was applied to the averaged data to remove any data gaps in the local time domain [*Zeng et al.*, 2008].

3. Results

[18] Figure 1 gives global maps of N_mF_2 calculated from COSMIC data for 4 local time bands from 1700 local time to 2100 local time. The data come from a 3 month period on the December solstice and so correspond to the southern summer. Figure 1a gives this map for the 1700–1800 local time band. This pattern is typical of the one described by *Lei et al.* [2007]. An equatorial anomaly is seen on both sides of the magnetic equator. The one in the northern (winter) hemisphere is weaker than the one in the southern (summer) hemisphere. Longitudinal structure is seen in these equatorial anomalies. The largest peak in the southern anomaly is over South America, with possible secondary peaks over the Indian and Pacific Oceans. The distribution of electron density in the northern equatorial anomaly appears more uniform, but this is partially a function of the wide range of electron densities that the green color represents. Apart from this, electron densities fall off toward higher latitudes, with the smallest values of N_mF_2 being found in the high latitudes of the northern, winter hemisphere. There is some longitudinal structure at higher latitudes. For example, N_mF_2 at 50°N maximizes over the Atlantic coast of North America.

Table 1. Approximate Time of Local Sunset at Various Latitudes for Mid-January Conditions[a]

Latitude	Sunset Time
65	14.2
60	15.1
55	15.7
50	16.2
45	16.5
40	16.7
25	17.3
15	17.6
0	18.
−15	18.4
−25	18.7
−40	19.3
−45	19.5
−50	19.8
−55	20.2
−60	20.8
−65	21.7

[a]Note that changes in Sun-Earth distance, eccentricity of Earth's orbit, etc., have not been taken into account.

[19] The first deviation from this pattern is seen in Figure 1b, which shows values of N_mF_2 in the 1800–1900 local time band. There is an increase in electron density in the middle latitudes west of South America which appears to be associated with the southern equatorial anomaly. Apart from this difference, the pattern is similar to that at the previous local time, albeit with reduced values of N_mF_2 globally. Maximum values of N_mF_2 occur in the southern equatorial over South America. Electron densities in the southern equatorial anomaly are larger than those in the north and there is some longitudinal structure in the anomalies. Longitudinally, electron densities in the middle latitudes also vary much as they did at 1700 local time, except for the aforementioned change that occurs over the South Pacific off Chile.

[20] A much greater change occurs in the 1900–2000 local time band (Figure 1c). The enhancement in electron densities that appears to be associated with the summer equatorial anomaly is far south over the Pacific Ocean west of Chile at this local time; its center is now between 45 and 60°S. The longitude region in which this occurs is fairly narrow, stretching only from about 100 to 140°W for the southernmost excursion. The shape of this excursion and its limited longitude range suggests a strong connection with the extension of the magnetic equator into the southern hemisphere. There appears to be continuity with the southern equatorial anomaly in this southern excursion, insofar as the anomaly appears to have been displaced southward in a band from north of New Zealand all the way to its southernmost location. Some of this may be inherent in the smoothing used in the analysis procedure (however, Figure 3 suggests otherwise), but the quite wide longitudinal extent of the excursions of the equatorial anomaly across the Pacific Ocean suggests continuity in the processes that are leading to the excursion. The electron densities associated with the earlier equatorial anomalies in this region are significantly depleted, suggesting that the equatorial anomaly has been displaced southward. Elsewhere in the world the equatorial anomalies continue to behave in much the same way as they did at earlier local times. The northern equatorial anomaly shows no changes in latitude; it just gets weaker. The southern equatorial anomaly over South America, the Atlantic and Indian Oceans also gets weaker but its latitude does not change. There are still significant longitudinal structures in the anomalies in these locations. Maxima are seen in the southern anomaly over South America, the west coast of Africa and Indonesia. The northern equatorial anomaly has a peak over South America, but other structure is difficult to discern.

[21] The band of enhanced electrons is far south of its normal position over the South Pacific in the 2000–2100 local time band (Figure 1d). The center of these enhanced electron densities is at 60°S in the Pacific Ocean west of Chile. The longitude of these enhancements is, in part, west of the normal location of the Weddell Sea anomaly, although the region of enhanced electrons does extend halfway across the Weddell Sea. A similar plot for the post midnight period, which is not presented in this paper, shows that this region of enhancements moves eastward through the night so that it covers the Weddell Sea region. The existence of this region of enhancements over the Bellingshausen and part of the Amundsen Sea soon after dusk does not indicate that they should have been observed by ground stations (approximate sunset time at ground level for various latitudes on 15 January are given in Table 1; F_2 peak sunset times are not given because, although light penetrates later at this level, very little ionizing radiation exists at 200 km after sunset on the ground). These enhanced densities occur only over water, where TOPEX observations have provided evidence of the ''Weddell Sea'' anomaly [*Horvath*, 2006]. These TOPEX observations show that the Weddell Sea anomaly extends into the South Pacific as far as 160°W, which is commensurate with the geographical distribution shown in this paper.

[22] The disturbed area also extends further across the South Pacific, albeit at lower latitudes. Electron densities are enhanced at middle latitudes over northern New Zealand. These enhancements appear to connect continuously with the region of enhanced densities at 60°S and 140°W. An ionosonde in northern New Zealand should observe a slower decrease in electron densities in the evening hours in summer than that which is seen at equivalent middle latitude stations at other locations (e.g., Camden, Australia). Elsewhere on the globe electron densities appear to be behaving as they did at earlier local times, although the magnitude of N_mF_2 is lower. The maximum in N_mF_2 in the southern anomaly has decreased considerably, leaving the peak over the West African coast as the largest one in the southern equatorial anomaly. There is another peak in the southern anomaly over Indonesia. The northern anomaly has diminished even more than the southern anomaly in this local time band.

[23] The behavior of N_mF_2 described above, has a counterpart in the behavior of h_mf_2, which may shed some light on the mechanism driving the changes. Figure 2 gives four plots of h_mf_2 in bands from 1700 to 1800 local time to 2000–2100 local time. The first local time band, from 1700 to 1800 local time, is shown in Figure 2a. The highest h_mf_2 values occur close to the magnetic equator, but not entirely coincident to it (see *Lei et al.* [2007] for possible reasons for this difference). The peak altitude is south of the magnetic equator from Africa all the way eastward across most of the

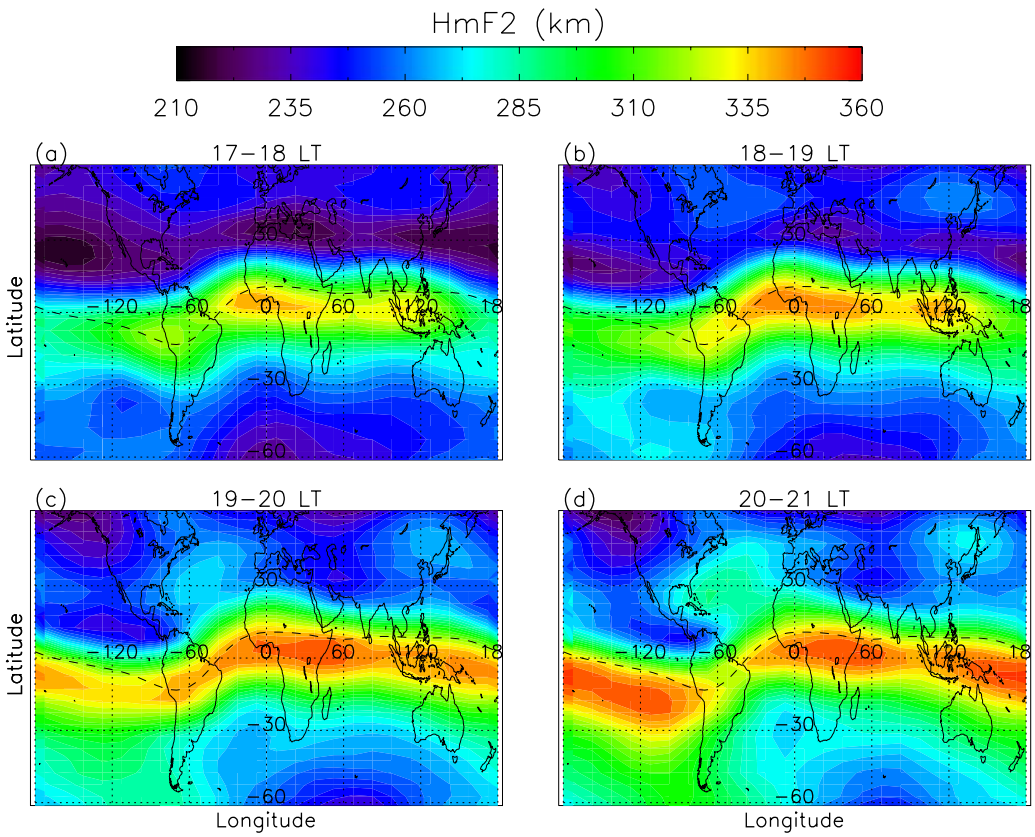

Figure 2. Global maps of h_mf_2 calculated from COSMIC data for four local time bands: (a) 1700–1800 local time, (b) 1800–1900 local time, (c) 1900–2000 local time, and (d) 2000–2100 local time.

Pacific Ocean. It is north of the magnetic equator over Brazil.

[24] The height of the F_2 peak decreases significantly as latitudes increase away from the magnetic equator. Lowest F_2 peak heights occur in a band in the northern hemisphere that is just poleward of the northern equatorial anomaly. Here peak heights can be as low as about 200 km; over 150 km lower than the greatest peak heights at the magnetic equator. There are considerable variations in h_mf_2 in the southern middle latitudes. Peak heights occur at altitudes of between about 250 km and 280 km over the South Pacific, whereas their altitude range is from about 230 to 250 km over the Indian Ocean. The values over the South Pacific are our main concern in this paper, so these will be discussed more completely in the subsequent paragraphs than those at other locations.

[25] Figure 2b is a map of h_mf_2 for the 1800 to 1900 local time band. Generally, h_mf_2 is occurring at higher altitudes over the whole globe at this time. The pattern is very similar to that in the previous local time band. Highest values occur near the magnetic equator and lowest values occur in the northern middle latitudes just poleward of the northern equatorial anomaly. Increases in h_mf_2 of the order of 20 to 30 km occur over the South Pacific, with a distinct tongue shape westward of the center of the enhancements of N_mF_2.

[26] The trends seen in the 1800 to 1900 local time band continue through into the 1900–2000 local time band (Figure 2c) Peak heights reach 300–310 km as far south as 50° S in the South pacific at about 120° W longitude. This represents an increase in altitude for the peak height of at least 50 km on the northern edge of the region of enhanced electron densities. The height increases are much smaller elsewhere in the southern middle latitudes, indicating that this increase in the South Pacific is part of the process that drives the displacement of the southern equatorial anomaly in this region.

[27] The last h_mf_2 plot shows that, for the 2000 to 2100 local time band (Figure 2d), the height increases in the South Pacific are even more dramatic. F_2 peak heights are above 325 km at latitudes as high as 30 S in the South Pacific and about 315 km at latitudes as high as 45 degrees. Peak heights thus increase by 60 to 70 km in the middle latitudes of this longitude sector. Increases in peak height are only about 30 km over middle latitude locations in other parts of the Earth.

[28] An obvious concern is that these changes in electron density that are observed over the South Pacific, Bellingshausen Sea and Weddell Sea are merely the result of the analysis procedures that were used. To counter this possibility we have looked at rawer forms of the data. Figure 3 presents the data in the 2000 to 2100 local time bin as dots. The location of these dots is determined by the position of the tangent point of the observation as it goes through the F_2 peak. Although these data have been inverted using the Abel inversion, no further analysis has been done on them. It can be seen that both the magnitudes of N_mF_2 and the pattern in which high electron densities are found at middle latitudes over the South Pacific Ocean occur in these data in

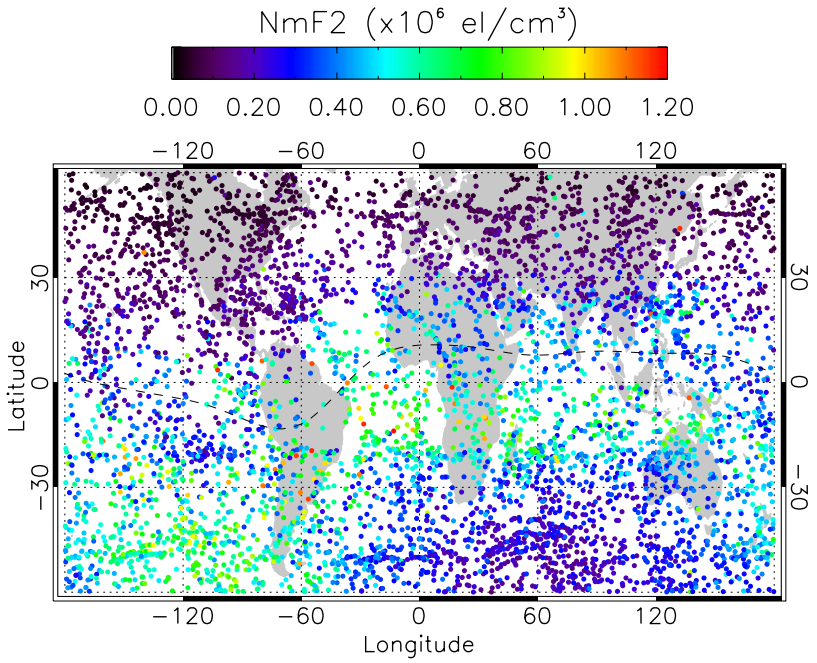

Figure 3. Individual data points of N_mF_2 from COSMIC satellites for the 2000–2100 local time bin.

much the same way as they do in the more highly analyzed data shown in Figures 1 and 2. In other words, the post processing of the observations did not change their main features, so the observed behavior is not just an artifact of the processing used.

4. Discussion

[29] The first question that arises when an unexpected phenomenon is seen in a data set is whether of not the observations reflect what is really happening. Typically it is impossible to absolutely prove that something is real, but a preponderance of evidence can be amassed to indicate that phenomenon is probably occurring.

[30] We have tried to amass such a preponderance of evidence in this paper to indicate that the dusk southward displacement of the southern equatorial anomaly in summer is a real phenomenon. There are several aspects to this process. The first is to determine whether the data set used reproduces is consistent in other places and times. In this case the morphology of the COSMIC data shows many features that are also seen in other data sets. Prior to the southward excursion of the southern equatorial anomalies, both sets of anomalies are located where they are expected to be relative to the magnetic equator. There is the expected seasonal variation in the magnitude and height of these anomalies and they exhibit longitudinal variations that have been seen in other data sets. Thus, the data set reproduces well-known features in the F_2-region ionosphere.

[31] The behavior of the ionosphere over the South Pacific that is seen in the COSMIC data is therefore the issue, rather than the entire data set. No previously published papers suggest that the equatorial anomaly can be displaced poleward in the way that is described in this paper. However, the end result of this displacement is to produce the Weddell Sea anomaly. This anomaly was first reported by *Bellchambers and Piggott* [1958], who used ionosonde measurements. It has also been measured by *Horvath* [2006] using TOPEX measurements. In other words, it has been observed using more than one technique and is an established phenomenon.

[32] The behavior of the F_2-region electron densities over the South Pacific is also supported by other measurements using a different sounding technique. Figure 8 in the *Horvath* [2006] paper indicates that the Weddell Sea anomaly is spread over much of the South Pacific near dusk and that the extension of the Weddell Sea anomaly to the equatorial anomaly over Indonesia is also present in these TOPEX data at all local times shown. The development of the Weddell Sea anomaly in the low and middle latitudes of the South Pacific in these data and the continued extension of the anomaly to the Indonesian sector may have not been discussed in that paper because of the large shift in local time as the satellite moves from the equator to high latitudes makes the data harder to interpret than the COSMIC data are.

[33] Given the obvious changes in the COSMIC and TOPEX observations that have been discussed in this paper, why would a synoptic feature as large as the displacement of enhanced electron densities that appear to be associated with the equatorial anomaly to the South Pacific Ocean at between 50 and 60 degrees not have been discussed previously in the literature, perhaps as early as the time of the discovery of the Weddell Sea anomaly in the late 1950s? The answer may lie in its location over a region of the Earth that cannot be observed from ground-based stations. Before the comprehensive satellite measurements from COSMIC and TOPEX became available, ionospheric observations over this region were limited to difficult analyses of along track measurements by one satellite. Even with satellite measurements it has not proved easy to separate local time and longitude effects in electron density measurements. The

comprehensive set of COSMIC observations has changed this situation.

[34] Even though the phenomenon seen here is supported by previous studies, there is still a concern that the analysis procedures may have introduced a false signal. The need to isolate local time, latitude, longitude and universal time effects means that there is considerable postprocessing of that data. For that reason we have presented the data in a rawer form (Figure 3) to show that this postprocessing has not changed the pattern significantly from that obtained by plotting the individual measurements.

4.1. Other Features of the F_2 Peak Electron Density Changes Over the South Pacific

[35] There are several features associated with the changes seen in F_2 peak electron density over the South Pacific which may help to identify the processes that drive the observed changes. The lifting up of the F_2 peak on the equatorward side of this anomaly involves ions moving to heights where recombination is significantly decreased, leading to enhanced electron densities. Ambipolar diffusion should shift this enhanced ionization downward and poleward.

[36] Another concern is why this phenomenon and the Weddell Sea anomaly occur in the southern summer. The illumination of the ionosphere as night is falling may be important. The longitudinal extent of this phenomenon is also very limited. It seems to be connected to the southward excursion of the magnetic equator. But it does not occur at the longitude of this southernmost excursion; instead it occurs on the western side of this bulge. There is no obvious reason why this area should be favored over others, but its location and the formation of the Weddell Sea anomaly in the same place for 50 years suggests that it is significant.

[37] The data provide a number of features that must be reconciled by any explanation of this displacement. First, the changes occur at dusk in a particular longitude sector. Second, they are associated with a region in which the magnetic field moves far further south of the geographic equator than it does anywhere else on the globe. Third, the displacement from the low latitudes to the high latitudes is very rapid. Fourth, there is a large h_mf_2 increase on the equatorward edge of the region of enhanced N_mF_2.

4.2. Possible Mechanisms for the Displacement

[38] It is worth considering various mechanisms that may produce this behavior. One way to change the height of the F_2 peak is through thermal expansion. As neutral temperatures increase the atmosphere swells. The height of the F_2 peak tends to remain on a constant pressure level [*Rishbeth and Edwards*, 1989, 1990], so it also increases. However, thermal expansion cannot explain what is seen in this paper for a number of reasons. First, there is no increase in electron density associated with thermal expansion. Second, temperatures are expected to decrease from about 1500 LT [e.g., see *Mayer et al.*, 1978], so the atmosphere is contracting rather than expanding. Third, there is no reason why thermal expansion would cause the latitude at which the electron densities peak to change suddenly.

[39] Other possible causes for the observed changes can be obtained from the O^+ continuity equation [e.g., see *Burns et al.*, 2007]. One possible mechanism is a change in neutral composition. If the proportion of the heavy molecular gases in a column of air is increased then the F_2 peak will move upward. However, the recombination rate for O^+ also increases in this scenario leading to a decrease in electron densities at the F_2 peak. Increases in O density compared with N_2 density can increase electron densities, but they should move the F_2 peak downward. So composition change does not seem to be a likely explanation for the behavior seen in Figures 1 and 2.

[40] Advection of ions by the neutral winds provides another possible scenario. Equatorward neutral winds blow up field lines, increasing the height of the F_2 peak and, as this peak has moved to heights where there is less recombination, increasing electron densities at the F_2 peak [e.g., *Prölss*, 1980]. However, neutral winds are primarily zonal at dusk in quiet geomagnetic conditions, where the observed displacement occurs [e.g., *Dickinson et al.*, 1981; *Burns et al.*, 1995], although these publications represent the general behavior of the meridional winds at dusk and they may not be applicable to the South Pacific region. Zonal neutral winds are not efficient at driving electrons up field lines (a little upward or downward motion can happen because the geographic and geomagnetic poles are at different locations), and the relatively smooth morphology of the neutral wind field in low and middle latitudes in quiet times argues against the neutral winds producing a relatively local change in electron density like the one reported here. There is a strong equatorward component to the neutral winds after midnight that is associated with the antisunward winds in the high-latitude convection zone [e.g., *Killeen and Roble*, 1988], but such a jet would argue for the winds forming an anomaly after midnight not at dusk.

[41] Two terms are left in the O^+ continuity equation that could explain this behavior: the electric field and ambipolar diffusion. One involves changes in electric fields. They could conceivably move ionization upward to where there is less loss and poleward. This could possibly cause the observed displacement, but the requirement for very rapid displacement is a concern. Also, there is no known change in electric field at these latitudes that could drive such a movement.

[42] The last possibility is that there is an enhancement of the downward ambipolar diffusion of ions and electrons from the plasmasphere. As the top-side ionosphere cools in the evening, its scale height decreases, moving plasma downward. As the O^+ pressure decreases at high altitudes, H^+ ions flow down from above. Charge exchange of the H^+ ions with atomic oxygen would fairly rapidly convert the H^+ ions to O^+, which are heavier and would be more strongly subject to gravity than H^+, and would therefore continue to diffuse downward. Such diffusion would lead to an increase in electron densities and an increase in the height of the F_2 peak, particularly at the equatorward edge of the disturbed region, where the projection of gravity along the magnetic field direction is weaker. Why should such an effect be particularly pronounced in the Weddell Sea region? Part of the answer may lie in the fact that magnetic-midlatitude electron temperatures in the lower plasmasphere are observed to cool in the summer evening more strongly in the southern hemisphere than in the northern hemisphere [*Kutiev et al.*,

2002], although these observations have not yet been analyzed for longitudinal variations.

4.3. Attempts to Model the Phenomenon

[43] An effort was made to model this behavior using the Coupled Magnetosphere Ionosphere Thermosphere model [*Wang et al.*, 2004; *Wiltberger et al.*, 2004], which includes interactive electric fields, but not an interactive plasmaspheric module. No feature like the one described over the South Pacific in this paper was found in the output from this model. Other modeling efforts that were reported by *Burns et al.* [2008] indicated that the modeled electron densities decayed more rapidly than those observed by ionosondes after dark in summer, suggesting that something is missing near dusk in the models in summer. The behavior described in this paper could possibly explain this model-data discrepancy.

5. Conclusions

[44] COSMIC data were analyzed here to study the diurnal variation of electron densities in the northern (southern) winter (summer) during quiet to moderate geomagnetic conditions. During daylight hours the data behaves just as it has done in numerous previous studies. Equatorial anomalies form on either side of the magnetic equator centered at about 20 degrees geomagnetic latitude. The heights of these peaks and their location also conform to the aforementioned previous studies.

[45] An odd thing happens near dusk, however. The enhanced electron densities that appear to be associated with the southern equatorial anomaly over the South Pacific Ocean occur far to the south at about 60° S. In tandem with this behavior the height of these enhanced electron densities increased on their equatorward edge. There is no evidence of issues in the analysis procedure or the data and these results are supported by independent measurements made by the TOPEX/Poseidon satellite. Furthermore, the end result of this behavior is to produce another anomaly that has been extensively described using data gathered from other, different observations. In other words there is strong evidence that the behavior described in this paper is real and that the high electron densities that appear to be associated with the southern equatorial anomaly occur far to the south at dusk over the South Pacific near the December solstice. Various physical mechanisms were considered in trying to explain this displacement, but they all had issues. Of those mechanisms considered, an evening downward flux of plasma from the plasmasphere has the potential to satisfy the observational constraints, and may be at least partly responsible for the phenomenon.

[46] **Acknowledgments.** This research was supported by the Center for Integrated Space Weather Modeling (CISM), which is funded by the STC program under agreement ATM-0120950. NCAR is supported by the National Science Foundation.

[47] Zuyin Pu thanks the reviewers for their assistance in evaluating this paper.

References

Beers, T. C., K. Flynn, and K. Gebhardt (1990), Measures of location and scale for velocities in clusters of galaxies-A robust approach, *Astron. J.*, *100*(1), 32–46, doi:10.1086/115487.

Bellchambers, W. H., and W. R. Piggott (1958), Ionospheric measurements made at Halley Bay, *Nature*, *182*, 1596–1597, doi:10.1038/1821596a0.

Bilitza, D. (2007), International Reference Ionosphere 2007, Natl. Space Sci. Data Cent., Greenbelt, Md. (Available at http://modelweb.gsfc.nasa.gov/ionos/iri.html)

Burns, A. G., T. L. Killeen, W. Deng, G. R. Carignan, and R. G. Roble (1995), Geomagnetic storm effects in the low- and middle-latitude upper thermosphere, *J. Geophys. Res.*, *100*, 14,673–14,691, doi:10.1029/94JA03232.

Burns, A. G., S. C. Solomon, W. Wang, and T. L. Killeen (2007), The ionospheric and thermospheric response to CMEs: Challenges and successes, *J. Atmos. Sol. Terr. Phys.*, *69*, 77–85, doi:10.1016/j.jastp.2006.06.010.

Burns, A. G., W. Wang, M. Wiltberger, S. C. Solomon, H. Spence, T. L. Killeen, R. E. Lopez, and J. E. Landivar (2008), An event study to provide validation of TING and CMIT geomagnetic middle-latitude electron densities at the F_2 peak, *J. Geophys. Res.*, *113*, A05310, doi:10.1029/2007JA012931.

Dickinson, R. E., E. C. Ridley, and R. G. Roble (1981), A three-dimensional general circulation model of the thermosphere, *J. Geophys. Res.*, *86*, 1499–1512, doi:10.1029/JA086iA03p01499.

Dudeney, J. R., and W. R. Piggott (1978), Antarctic ionospheric research, in *Upper Atmosphere Research in Antarctica*, *Antarct. Res. Ser.*, vol. 29, edited by L. J. Lanzerotti and C. G. Park, pp. 200–235, AGU, Washington, D. C.

Hajj, G. A., and L. J. Romans (1998), Ionospheric electron density profiles obtained with the Global Positioning System: Results from the GPS/MET experiment, *Radio Sci.*, *33*, 175–190.

Horvath, I. (2006), A total electron content space weather study of the nighttime Weddell Sea Anomaly of 1996/1997 southern summer with TOPEX/Poseidon radar altimetry, *J. Geophys. Res.*, *111*, A12317, doi:10.1029/2006JA011679.

Jee, G., A. G. Burns, W. Wang, S. C. Solomon, R. W. Schunk, L. Scherliess, D. C. Thompson, J. J. Sojka, and L. Zhu (2007), Duration of an ionospheric data assimilation initialization of a coupled thermosphere-ionosphere model, *Space Weather*, *5*, S01004, doi:10.1029/2006SW000250.

Killeen, T. L., and R. G. Roble (1988), Thermosphere dynamics driven by magnetospheric sources: Contributions from the first five years of the Dynamics Explorer program, *Rev. Geophys. Space Phys.*, *26*(2), 329–367, doi:10.1029/RG026i002p00329.

Kumar, M. (2006), New satellite constellation uses radio occultation to monitor space weather, *Space Weather*, *4*, S05003, doi:10.1029/2006SW000247.

Kutiev, I., K. I. Oyama, and T. Abe (2002), Analytical representation of the plasmasphere electron temperature distribution based on Akebono data, *J. Geophys. Res.*, *107*(A12), 1459, doi:10.1029/2002JA009494.

Lei, J., et al. (2007), Comparison of COSMIC ionospheric measurements with ground-based observations and model predictions: Preliminary results, *J. Geophys. Res.*, *112*, A07308, doi:10.1029/2006JA012240.

Mayer, H. G., I. Harris, and N. W. Spencer (1978), Some properties of upper atmosphere dynamics, *Rev. Geophys. Space Phys.*, *16*, 539–565, doi:10.1029/RG016i004p00539.

Penndorf, R. (1965), The average ionospheric conditions over the Antarctic, in *Geomagnetism and Aeronomy*, *Antarct. Res. Ser*, vol. 4, edited by A. H. Waynick, pp. 1–45, AGU, Washington, D. C.

Prölss, G. W. (1980), Magnetic storm associated perturbation of the upper atmosphere: Recent results obtained by satellite-borne gas analyzers, *Rev. Geophys. Space Phys.*, *18*, 183–202, doi:10.1029/RG018i001p00183.

Rishbeth, H., and R. Edwards (1989), The isobaric F2-layer, *J. Atmos. Terr. Phys.*, *51*, 321–338, doi:10.1016/0021-9169(89)90083-4.

Rishbeth, H., and R. Edwards (1990), Modeling the F2 layer peak height in terms of atmospheric pressure, *Radio Sci.*, *25*, 757–769, doi:10.1029/RS025i005p00757.

Rishbeth, H., and O. K. Garriott (1969), *Introduction to Ionospheric Physics*, Academic, San Diego, Calif.

Rocken, C., Y.-H. Kuo, W. Schreiner, D. Hunt, S. Sokolovskiy, and C. McCormick (2000), COSMIC system description, *Terr. Atmos. Ocean Sci.*, *11*, 21–52.

Schreiner, W. S., S. V. Sokolovskiy, C. Rocken, and D. C. Hunt (1999), Analysis and validation of GPS/MET radio occultation data in the ionosphere, *Radio Sci.*, *34*(4), 949–966, doi:10.1029/1999RS900034.

Wang, W., M. Wiltberger, A. G. Burns, S. Solomon, T. L. Killeen, N. Maruyama, and J. Lyon (2004), Initial results from the CISM coupled magnetosphere-ionosphere-thermosphere (CMIT) model: Thermosphere ionosphere responses, *J. Atmos. Sol. Terr. Phys.*, *66*, 1425–1442, doi:10.1016/j.jastp.2004.04.008.

Wiltberger, M., W. Wang, A. Burns, S. Solomon, J. G. Lyon, and C. C. Goodrich (2004), Initial results from the coupled magnetosphere ionosphere thermosphere model: Magnetospheric and ionospheric responses, *J. Atmos. Sol. Terr. Phys.*, *66*, 1411–1444, doi:10.1016/j.jastp.2004.03.026.

Zeng, Z., A. G. Burns, W. Wang, J. Lei, S. C. Solomon, S. Syndergaard, L. Qian, and Y.-H. Kuo (2008), Ionospheric annual asymmetry observed by the COSMIC radio occultation measurements and simulated by the TIEGCM, *J. Geophys. Res.*, *113*, A07305, doi:10.1029/2007JA012897.

A. G. Burns, T. L. Killeen, A. D. Richmond, S. C. Solomon, and W. Wang, High Altitude Observatory, National Center for Atmospheric Research, Boulder, CO 80307-3000, USA. (aburns@ucar.edu)

Y.-H. Kuo, Mesoscale and Microscale Meteorology Division, National Center for Atmospheric Research, Boulder, CO 80307-3000, USA.

J. Lei, Aerospace Engineering Sciences Department, University of Colorado, Boulder, CO 80309-0429, USA.

Z. Zeng, Department of Earth and Ocean Sciences, University of British Columbia, 2329 West Mall, Vancouver, BC V6T 1Z4, Canada.